NACA

RESEARCH MEMORANDUM

THE SUBSONIC LATERAL AND LONGITUDINAL STATIC STABILITY

CHARACTERISTICS UP TO LARGE ANGLES OF SIDESLIP

FOR A TRIANGULAR-WING AIRPLANE MODEL

HAVING A VENTRAL FIN

By Donald A. Buell and Bruce E. Tinling

Ames Aeronautical Laboratory
Moffett Field, Calif.

NATIONAL ADVISORY COMMITTEE
FOR AERONAUTICS

WASHINGTON

October 25, 1956

NATIONAL ADVISORY COMMITTEE FOR AERONAUTICS

RESEARCH MEMORANDUM

THE SUBSONIC LATERAL AND LONGITUDINAL STATIC STABILITY

CHARACTERISTICS UP TO LARGE ANGLES OF SIDESLIP

FOR A TRIANGULAR-WING AIRPLANE MODEL

HAVING A VENTRAL FIN

By Donald A. Buell and Bruce E. Tinling

SUMMARY

Wind-tunnel tests were conducted to determine the effects of a ventral fin on the static characteristics of a triangular-wing airplane model. Data were obtained for angles of sideslip up to 18° at angles of attack of 0°, 6°, 12°, and 18° at Mach numbers from 0.25 to 0.94.

The results of the tests indicated that the ventral fin did not produce as much yawing moment per unit of exposed area at any angle of sideslip as the vertical tail. There were no important effects of sideslip or of the ventral fins on the longitudinal characteristics.

INTRODUCTION

One of the problems facing designers of high-performance airplanes is the prevention of abruptly divergent motions of the airplane in a rolling maneuver. The problem has been analyzed in reference 1 where it was shown that roll-induced instability might occur if the rolling frequency exceeds the lower of the pitching and yawing natural frequencies of the nonrolling airplane. One of the airplanes in which this coupled motion has been experienced is a triangular-wing airplane similar to the model described in reference 2. The flight experience with this airplane has been reported in reference 3. This airplane has most of the mass distributed lengthwise within its fuselage and has low directional stability, both of which cause low values of yawing natural frequency and thus restrict the rate of roll which may be used safely in a maneuver.

The triangular-wing airplane model of reference 2 was therefore selected for studies of a ventral fin, which was intended as a device

to improve the stability characteristics of the airplane in a rolling
maneuver. It was anticipated that the fin would have an increasing con-
tribution to the directional stability with increasing angle of sideslip
but would have little effect on the aerodynamic characteristics at small
angles of sideslip. The resulting increase in the yawing natural fre-
quency of the nonrolling airplane as the sideslip angle is increased
would be expected to increase the roll rate at which large divergencies
in sideslip would be experienced. The effect of the ventral fin on the
coupled motion was studied by computing the response to steady rolling
of the airplane free to pitch and yaw.

Other objectives of the tests were to extend the data on the lateral
and longitudinal characteristics of the model of reference 2 to large
angles of sideslip, and to find the effect of sideslip on the directional
stability and damping in yaw measured during an oscillatory motion. The
tests were conducted in the Ames 12-foot pressure wind tunnel at Mach
numbers up to 0.94 and Reynolds numbers up to 4.9 million.

NOTATION

The forces and moments on the model are referred to the stability
system of axes shown in figure 1. The coefficients are defined as follows:

C_D' drag coefficient, $\dfrac{\text{drag}}{\frac{1}{2}\,\rho V^2 S}$

C_L lift coefficient, $\dfrac{\text{lift}}{\frac{1}{2}\,\rho V^2 S}$

C_m pitching-moment coefficient, $\dfrac{\text{pitching moment}}{\frac{1}{2}\,\rho V^2 S \bar{c}}$

C_n yawing-moment coefficient, $\dfrac{\text{yawing moment}}{\frac{1}{2}\,\rho V^2 S b}$

C_Y side-force coefficient, $\dfrac{\text{side force}}{\frac{1}{2}\,\rho V^2 S}$

C_l rolling-moment coefficient, $\dfrac{\text{rolling moment}}{\frac{1}{2}\rho V^2 Sb}$

$\Delta C_{n,fin}$ yawing-moment coefficient due to fin, $C_{n,fin\ on} - C_{n,fin\ off}$

C_{m_q} $\dfrac{\partial C_m}{\partial(q\bar{c}/2V)}$, per radian

C_{m_α} $\dfrac{\partial C_m}{\partial\alpha}$, per deg

$C_{m_{\dot\alpha}}$ $\dfrac{\partial C_m}{\partial(\dot\alpha\bar{c}/2V)}$, per radian

C_{n_r} $\dfrac{\partial C_n}{\partial(rb/2V)}$, per radian

C_{n_β} $\dfrac{\partial C_n}{\partial\beta}$, per deg

$C_{n_{\dot\beta}}$ $\dfrac{\partial C_n}{\partial(\dot\beta b/2V)}$, per radian

The additional symbols used are defined as follows:

b wing span

c wing chord

$\bar{c}$ mean aerodynamic chord

M free-stream Mach number

q pitching angular velocity

r yawing angular velocity

R Reynolds number, based on wing mean aerodynamic chord

S wing area

V   free-stream velocity

α angle of attack, deg

$\dot{\alpha}$ time rate of change of angle of attack

β angle of sideslip, deg

$\dot{\beta}$ time rate of change of angle of sideslip

ρ air density

MODEL AND APPARATUS

Details of the model geometry are given in the three-view drawing
of figure 2 and in table I. The model is more fully described in refer-
ence 2. In the present investigation provision was made to mount ventral
fins either in the plane of symmetry or in planes 40° from the plane of
symmetry. Fins of several sizes and shapes were tested, with the emphasis
of this report placed on the fin shown in figure 2.

For static-force tests, the model was mounted on a four-component
strain-gage balance enclosed by the model body. The balance was supported
by a 4-inch-diameter sting, which could be deflected in a vertical plane,
permitting variations in angle of attack (wings horizontal) or in angle
of sideslip (wings vertical). Stings bent at various angles in the hori-
zontal plane were used to attain various combinations of the angles of
attack and sideslip. The angle in the vertical plane was indicated by a
pendulum-type instrument mounted in the model body. A photograph of the
model mounted in the wind tunnel is shown in figure 3.

For oscillation tests, the model was mounted on a single-degree-of-
freedom oscillatory apparatus described in reference 2. This consists
of a mechanism which produces an oscillation of the model and is instru-
mented to measure the damping and restoring moments on the model.

TESTS

The major portion of the investigation consisted of yawing-moment,
rolling-moment, and side-force measurements with the model at an angle
of attack of 0°, 6°, 12°, or 18°. However, at the highest test Mach
number (0.94) the angle of attack was limited to 6° by choking of the
wind tunnel. The angle of sideslip was varied from -8° to 18°. The
Reynolds number for this series of tests was 2.7 million at a Mach number
of 0.25, and 1.5 million at Mach numbers of 0.80, 0.90, and 0.94. The

model was tested with various combinations of the wing, the ventral fin, the wing fences, and the body-tail assembly. A limited number of static-force measurements were made at a higher Reynolds number (4.9 million) at a Mach number of 0.46. For these tests the variables were size, shape, and position of the ventral fin. Tests were also conducted to determine the longitudinal characteristics of the model at sideslip angles up to 18°.

In another series of tests, the model was oscillated in yaw at frequencies of from 6 to 7 cycles per second, and measurements were made of the static directional stability and the damping in yaw. These tests were made at 0° angle of attack with a variation in sideslip angle. The sideslip angle was limited at the higher Mach numbers by static deflection of the flexure pivots upon which the model was mounted. Testing was terminated when it was impossible to maintain an oscillation amplitude of approximately 1.5°. The Reynolds numbers and Mach numbers duplicated those of the major series of static-force tests. The configuration changes were limited to the addition of the ventral fin to the wing-body-tail assembly.

CORRECTIONS TO DATA

For the longitudinal data, corrections were made to the angle of attack and to the drag coefficient to compensate for the induced effects of the tunnel walls. The values, computed by the method of reference 4, were:

$$\Delta\alpha = 0.25 \; C_L, \; \text{deg}$$

$$\Delta C_D' = 0.0043 \; C_L^2$$

No effort was made to modify the correction for the off-center position of the model in the tunnel.

The stated angle of attack for the lateral data, which were obtained with sideslip as a variable, is equal to the sting bend angle. A calibration of the sting and its support indicated deflections of the order of 0.3° for the maximum load imposed during the wind-tunnel tests. Hence, the stated angle of attack for the lateral data may be in error by as much as 0.5° when the sting deflection and tunnel-wall corrections are taken into account.

The data were corrected by the method of reference 5 to take account of the effects of constriction due to the tunnel walls. This correction amounted to less than 2 percent of the dynamic pressure at the highest test Mach number of 0.94.

The drag data were adjusted to correspond to those of a model with a base pressure equal to free-stream static pressure.

DISCUSSION

Experimental Results

The results of preliminary tests conducted for purposes of selecting a ventral fin for further study are presented in figure 4. These results revealed that all of the fins produced the desired shape of the curve of yawing moment due to the fin versus sideslip, but that the departure from linearity and the resultant change in yawing-moment coefficient in each case was small. The largest of the four fins was selected for further study. This fin provided more yawing moment per unit of exposed area than any of the others. Test results (not presented) showed that two fins placed $40°$ from the plane of symmetry were less effective than a single fin having the same plan form placed in the plane of symmetry.

The results of yawing-moment measurements with the fin on and with the fin removed are presented in figure 5. Similar results obtained with the wing removed are presented in figure 6. It may be noted that these data indicate the model to be somewhat asymmetrical. This asymmetry was found to be the result of a slight bend, or perhaps warpage, of the vertical tail. This asymmetry did not exist during the tests reported in reference 2. The net yawing moment due to the ventral fin for Mach numbers up to 0.94 is summarized in figure 7. These data indicate the effect of the fin to be approximately the same for all angles of attack and Mach numbers when the wing was on. Comparison of these data ($R = 2.7 \times 10^6$ at $M = 0.25$ and 1.5×10^6 at $M = 0.80$ to 0.94) with those of figure 4 ($R = 4.9 \times 10^6$) indicates the effect of Reynolds number between 1.5 and 4.9 million to be small. Removing the wing generally increased the effectiveness of the fins at all but the highest angle of attack.

The data with the tail removed presented in reference 2 were used as a base from which to compare the increment in yawing moment due to the vertical tail and that due to the ventral fin. The comparison was made for $10°$ of sideslip at $6°$ angle of attack at a Mach number of 0.80. It was found that with the wing on, the fin was roughly 40 percent as effective per unit of exposed area as the vertical tail in producing yawing moment. When the wing was removed, the ventral fin, per unit of area, was 90 percent as effective as the vertical tail. At higher angles of sideslip, this comparison is more favorable to the ventral fin since its effectiveness increases with increasing sideslip, whereas that of the vertical tail decreases. For example, at $16°$ of sideslip, the fin was about 50 percent as effective per unit area as the vertical tail when the wing was on and about 150 percent when the wing was removed.

It was assumed for purposes of making the comparison that the variations of yawing-moment coefficient with sideslip for the body-wing combination and for the body alone were identical and linear. Data presented in reference 2 for 6° angle of attack indicate these assumptions to be reasonable.

The ventral fin compares more favorably with the vertical tail when the wing is removed for two reasons. The first of these is the favorable interference effect of the wing which improves the effectiveness of the vertical tail by reducing the sidewash at the vertical tail. The second is that a large part of the yawing moment due to the fin depends on its spoiling effect on the flow on the lee side of the fuselage. When a surface, such as a wing or horizontal tail, is placed above the ventral fin, the area over which this effect will exist will be limited. It would appear, therefore, that a ventral fin would be most advantageous on airplane configurations which have no horizontal surfaces mounted on the fuselage near the fin.

The measured directional stability due to the fins is seen in figure 8 to have approximately the same value from oscillatory tests as from static tests. (The value of C_{n_β} for the static test results was taken as the average over a range of sideslip angles extending 1.5° on either side of the specified sideslip angle. This is approximately the amplitude of the yawing oscillation employed during the oscillation tests.) Measurements of the damping in yaw indicate no significant effect of the ventral fin on this parameter (see fig. 9). It should be noted that the model had a large amount of directional instability with its tail removed (see ref. 2), so that the fin contribution was only a minute proportion of the tail contribution to the directional stability. Thus, the contribution of the fin to the damping in yaw would also be expected to be extremely small.

The dihedral effect was increased slightly (i.e., the rate of change of C_l with β was made more negative) by the fin at small angles of attack as is illustrated in figure 10. This change is in the opposite sense to that which would be expected from a fin mounted on the lower side of the fuselage. Apparently, the action of the fin in spoiling the flow over the lee side of the fuselage also reduced the pressures over the lower surface of the inner part of the lee wing panel. At higher angles of attack, the rolling moment caused by this effect was equal to or smaller than the rolling moment contributed by direct forces on the fin.

The effect of the ventral fin on the side-force coefficient is shown in figure 11. As would be anticipated from the yawing-moment results, addition of the fins caused very little change in side force.

The longitudinal characteristics, presented in figure 12, were little affected by the ventral fin or by 18° of sideslip.

During the course of the investigation, it was noted that large non-linear variations of rolling moment with sideslip occurred at an angle of attack of 12° at Mach numbers of 0.80 and 0.90. (See figs. 10(b) and 10(c).) A reduction of directional stability also occurred under these conditions. (See figs. 5(b) and 5(c).) These nonlinearities were not detected during the tests reported in reference 2 since data were obtained for sideslip angles of only 0° and 6° at 12° angle of attack. The limited data of reference 2, however, do show that wing fences increase the dihedral effect and improve the directional stability at this angle of attack. Further tests were made, therefore, to find the effect of wing fences on the lateral characteristics at 12° angle of attack. The results indicate that addition of the fences eliminated the large nonlinear variation of rolling moment with sideslip and increased the yawing moment due to sideslip at all sideslip angles up to 18°.

Calculations of Airplane Response to Steady Rolling

As noted previously, the ventral fin is not so effective per unit of exposed area in producing yawing moment as the vertical tail. It would seem, then, that the use of a ventral fin to alleviate inertial coupling would be limited to cases where it is impractical to enlarge the vertical tail. The possible effects of a ventral fin on inertial coupling were studied by calculating the response to steady rolling of an airplane free to pitch and yaw. This response was calculated by applying the Laplace transformation to the equations developed by Phillips in reference 1 for a steadily rolling airplane. The use of the Laplace transformation to calculate the motion of a rigid body is described in reference 6. The final expressions for angle of attack and sideslip are given in the appendix.

The use of two degrees of freedom, rather than four, to describe the motion of a steadily rolling aircraft involves the deletion of the terms containing normal force due to angle of attack and side force due to side-slip from the final expressions for angle of attack and angle of side-slip. As noted in reference 7, deletion of these terms will change the damping of the system, but will not change the characteristics of the coupled motion.

The calculations were made for an airplane having dimensions 13-1/3 times those of the model and having the assumed mass and aerodynamic characteristics listed in table II. The airplane was assumed to be initially in steady level flight at an angle of attack of 5.6°, at a Mach number of 0.8 and an altitude of 40,000 feet. The nonlinear variation of yawing-moment coefficient with sideslip angle was approximated with linear segments as illustrated in figure 13. This required three separate computations for each curve, the initial conditions for each of the last two being those which prevailed at $\beta = 1°$ and $\beta = 8°$, respectively.

The linear segment chosen for β greater than 8° does not approximate the experimental data for an angle of attack of 6°. (See variations A and C in fig. 13.) The slope of the curve for these sideslip angles was reduced to approximate the slope at an angle of attack of 0° since it was found that the angle of attack was approaching 0° by the time the motion had progressed to an angle of sideslip much greater than 8°.

The maximum excursion in angle of attack $\Delta\alpha_{max}$ and in sideslip β_{max} for each of the calculated time histories for 360° of roll are shown in the lower part of figure 13. The results indicate that the fins reduced the peak excursion in sideslip by about 20 percent and increased the roll rate for the peak excursion in sideslip by about 10° per second (compare response for variations A and C). The computations were not extended to a roll rate high enough to find the peak excursion in angle of attack, but the reductions in the angle of attack excursion for a given roll rate were as great as 6°.

Computations were also made for a linear variation of yawing moment with sideslip for sideslip angles greater than 1° (variations B and D in fig. 13) to compare with the other results to indicate the effect of the decrease in directional stability at high angles of sideslip. For the case with the fins off (curves A and B in fig. 13), considering a linear variation of yawing moment with sideslip reduced the peak excursion in sideslip by slightly more than 2°. The effect for the case with the fins on was to reduce the peak excursion in sideslip by only 1°.

CONCLUDING REMARKS

The results of wind-tunnel tests at subsonic speeds have shown that, for a triangular-wing airplane model, a ventral fin was not so effective per unit of exposed area as a vertical tail in producing yawing moment at any angle of sideslip up to 18°. However, the effectiveness of the fin was increased considerably when the wing was removed, indicating that a ventral fin may be more effective on configurations which have no horizontal surfaces close enough to interfere with the fin's spoiling action on the flow around the fuselage. Neither the ventral fin nor 18° of sideslip were found to have any important effect on the static longitudinal stability.

Calculations were made of the response to steady rolling during a 360° roll of an airplane free to pitch and to yaw. These calculations, which are for a Mach number of 0.80 and an altitude of 40,000 feet, showed that a ventral fin (with an area about 1/4 of the exposed tail area) reduced the peak excursion in sideslip by about 20 percent. The calculations also showed that the large reduction in directional stability which occurred at an angle of sideslip of about 8° caused only small

increases in the peak excursion during a 360° roll over that calculated for a linear variation of yawing moment with sideslip angle.

Ames Aeronautical Laboratory
     National Advisory Committee for Aeronautics
          Moffett Field, Calif., August 6, 1956

APPENDIX

CALCULATION OF THE MOTION OF A STEADILY ROLLING AIRPLANE FREE TO

PITCH AND TO YAW BY MEANS OF THE LAPLACE TRANSFORMATION

The equations of motion for a steadily rolling aircraft given by Phillips in reference 1 have been modified to allow for the inclusion of an initial yawing moment and pitching moment. The equations, which are referred to a principal system of axes, are as follows:

$$\ddot{\theta} - 2p_o\dot{\psi} - p_o{}^2\theta + 2\zeta_\theta\omega_\theta p_o(\dot{\theta} - p_o\psi) + \omega_\theta{}^2 p_o{}^2\theta - \frac{M_o}{I_Y} = 0 \quad (1)$$

$$\ddot{\psi} + p_o\dot{\theta} + (p_o{}^2\psi - p_o\dot{\theta})F + 2\zeta_\psi\omega_\psi p_o(\dot{\psi} + p_o\theta) + \omega_\psi{}^2 p_o{}^2\psi - \frac{N_o}{I_Z} = 0 \quad (2)$$

The notation which is identical to that used in reference 1 is as follows:

θ pitch angle, radians (equivalent to angle of attack, α, for system with two degrees of freedom)

ψ yaw angle, radians (approximately equivalent to the negative of the angle of sideslip, $-\beta$)

φ roll angle, radians

p_o steady roll rate, radians/sec

ζ_θ pitch damping ratio, $\dfrac{-M_q}{2\sqrt{-M_\theta I_Y}}$

ζ_ψ yaw damping ratio, $\dfrac{-N_r}{2\sqrt{-N_\psi I_Z}}$

$\omega_\theta p_o$ nonrolling natural pitch frequency, $\sqrt{\dfrac{-M_\theta}{I_Y}}$, radians/sec

$\omega_{\psi}p_o$ nonrolling natural yaw frequency, $\sqrt{\dfrac{-N_{\psi}}{I_Z}}$, radians/sec

F inertia factor, $\dfrac{I_X - I_Y}{I_Z}$

M_o intercept of curve of M vs. α at $\alpha = 0$

N_o intercept of curve of N vs. β at $\beta = 0$

where

M pitching moment, ft-lb

N yawing moment, ft-lb

M_{θ} pitching moment due to pitch angle, $\dfrac{\partial M}{\partial \theta}$

M_q pitching moment due to pitching velocity, $\dfrac{\partial M}{\partial q}$

N_{ψ} yawing moment due to yaw, $\dfrac{\partial N}{\partial \psi}$

N_r yawing moment due to yawing velocity, $\dfrac{\partial N}{\partial r}$

I_X moment of inertia about the roll axis

I_Y moment of inertia about the pitch axis

I_Z moment of inertia about the yaw axis

$(\dot{\ })$ first derivative with respect to time

$(\ddot{\ })$ second derivative with respect to time

$(\ )_o$ initial conditions

Equations (1) and (2) were modified by expressing time nondimensionally in terms of the frequency of the steady rolling motion. The calculations necessary to compute the airplane motions were then performed in the manner indicated in reference 6. It should be noted that, in the

method used, all of the roots of the stability quartic are assumed to be distinct. The solution of the equations for pitch and yaw angle can be expressed as

$$\theta = A_1 e^{\varphi \lambda_1} + A_2 e^{\varphi \lambda_2} + A_3 e^{\varphi \lambda_3} + A_4 e^{\varphi \lambda_4} + A_5 \tag{3}$$

$$\psi = B_1 e^{\varphi \lambda_1} + B_2 e^{\varphi \lambda_2} + B_3 e^{\varphi \lambda_3} + B_4 e^{\varphi \lambda_4} + B_5 \tag{4}$$

where φ is the roll angle and λ_n are the roots of the stability quartic $A\lambda^4 + B\lambda^3 + C\lambda^2 + D\lambda + E = 0$ given in reference 1.

The constants A_n and B_n are calculated as follows:

$$A_n = \frac{a_0 \lambda_n^4 + a_1 \lambda_n^3 + a_2 \lambda_n^2 + a_3 \lambda_n + a_4}{5A\lambda_n^4 + 4B\lambda_n^3 + 3C\lambda_n^2 + 2D\lambda_n + E} \tag{5}$$

$$B_n = \frac{b_0 \lambda_n^4 + b_1 \lambda_n^3 + b_2 \lambda_n^2 + b_3 \lambda_n + b_4}{5A\lambda_n^4 + 4B\lambda_n^3 + 3C\lambda_n^2 + 2D\lambda_n + E} \tag{6}$$

The fifth root in the transformed equation is zero and hence:

$$A_5 = \frac{a_4}{E}$$

$$B_5 = \frac{b_4}{E}$$

When the transient motion is stable, the terms a_4/E and b_4/E correspond to the steady-state condition.

The following equations were used to evaluate the constants required to calculate A_n and B_n:

$$A = 1$$

$$B = 2\zeta_\theta \omega_\theta + 2\zeta_\psi \omega_\psi$$

$$C = \omega_\theta^2 + \omega_\psi^2 + 4\zeta_\theta \omega_\theta \zeta_\psi \omega_\psi + (1 - F)$$

$$D = 2\zeta_\theta \omega_\theta + 2\zeta_\psi \omega_\psi + 2\omega_\theta^2 \zeta_\psi \omega_\psi + 2\omega_\psi^2 \zeta_\theta \omega_\theta$$

$$E = (\omega_\theta^2 - 1)(\omega_\psi^2 + F) + 4\zeta_\theta\omega_\theta\zeta_\psi\omega_\psi$$

$$a_0 = \theta_0$$

$$a_1 = \dot\theta_0 + \theta_0(2\zeta_\psi\omega_\psi + 2\zeta_\theta\omega_\theta)$$

$$a_2 = \theta_0[4\zeta_\theta\omega_\theta\zeta_\psi\omega_\psi + \omega_\psi^2 + F + 2(1 - F)] + \dot\theta_0(2\zeta_\psi\omega_\psi) + \psi_0(2\zeta_\theta\omega_\theta) +$$

$$2\dot\psi_0 + \frac{M_0}{I_Y p_0^2}$$

$$a_3 = \theta_0(2\zeta_\theta\omega_\theta\omega_\psi^2 + 2\zeta_\theta\omega_\theta) + \dot\theta_0(\omega_\psi^2 + F) - \psi_0[2(\omega_\psi^2 + F) - 4\zeta_\theta\omega_\theta\zeta_\psi\omega_\psi] +$$

$$\dot\psi_0(2\zeta_\theta\omega_\theta) + 2\left(\frac{N_0}{I_Z p_0^2}\right) + 2\zeta_\psi\omega_\psi\left(\frac{M_0}{I_Y p_0^2}\right)$$

$$a_4 = \frac{M_0}{I_Y p_0^2}(\omega_\psi^2 + F) + 2\zeta_\theta\omega_\theta\left(\frac{N_0}{I_Z p_0^2}\right)$$

$$b_0 = \psi_0$$

$$b_1 = \psi_0(2\zeta_\theta\omega_\theta + 2\zeta_\psi\omega_\psi) + \dot\psi_0$$

$$b_2 = -\theta_0(2\zeta_\psi\omega_\psi) - \dot\theta_0(1 - F) + \psi_0[(\omega_\theta^2 - 1) + 4\zeta_\theta\omega_\theta\zeta_\psi\omega_\psi + 2(1 - F)] +$$

$$\dot\psi_0(2\zeta_\theta\omega_\theta) + \frac{N_0}{I_Z p_0^2}$$

$$b_3 = \theta_0[(\omega_\theta^2 - 1)(1 - F) - 4\zeta_\psi\omega_\psi\zeta_\theta\omega_\theta] - \dot\theta_0(2\zeta_\psi\omega_\psi) + \psi_0(2\omega_\theta^2\zeta_\psi\omega_\psi + 2\zeta_\psi\omega_\psi) +$$

$$\dot\psi_0(\omega_\theta^2 - 1) + 2\zeta_\theta\omega_\theta\frac{N_0}{I_Z p_0^2} - (1 - F)\frac{M_0}{I_Y p_0^2}$$

$$b_4 = (\omega_\theta^2 - 1)\frac{N_0}{I_Z p_0^2} - \frac{M_0}{I_Y p_0^2}(2\zeta_\psi\omega_\psi)$$

REFERENCES

1. Phillips, William H.: Effect of Steady Rolling on Longitudinal and
    Directional Stability. NACA TN 1627, 1948.

2. Beam, Benjamin H., Reed, Verlin D., and Lopez, Armando E.: Wind-
    Tunnel Measurements at Subsonic Speeds of the Static and Dynamic-
    Rotary Stability Derivatives of a Triangular-Wing Airplane Model
    Having a Triangular Vertical Tail. NACA RM A55A28, 1955.

3. Sisk, Thomas R., and Andrews, William H.: Flight Experience With a
    Delta-Wing Airplane Having Violent Lateral-Longitudinal Coupling
    in Aileron Rolls. NACA RM H55H03, 1955.

4. Glauert, H.: The Elements of Aerofoil and Airscrew Theory.
    MacMillan Co., 1943, pp. 189-198.

5. Herriot, John G.: Blockage Corrections for Three-Dimensional-Flow
    Closed Throat Wind Tunnels With Consideration of the Effect of
    Compressibility. NACA Rep. 995, 1950.

6. Campbell, John P., and McKinney, Marion O.: Summary of Methods for
    Calculating the Dynamic Lateral Stability and Response and for
    Estimating Lateral Stability Derivatives. NACA Rep. 1098, 1952.

7. Sternfield, Leonard: A Simplified Method of Determining the Transient
    Motion in Angle of Attack and Sideslip During a Constant Rolling
    Maneuver. NACA RM L56F04, 1956.

TABLE I.- MODEL DIMENSIONS

Wing (basic plan form, leading and trailing edges extending to vertex
    and to plane of symmetry)
    Span, b, ft 2.86
    Area, S, sq ft 3.72
    Mean aerodynamic chord, $\bar{c}$, ft 1.74
    Aspect ratio 2.20
    Leading edge sweep, deg   60
    True taper ratio (with cropped tips) 0.03
    Incidence, deg   0
    Dihedral, deg   0
    Airfoil section . . . . NACA 0004-65
    Vertical location (chord plane below moment center, ft . . .   0.05
Vertical tail (basic triangle projected to body center line)
    Span, ft 0.91
    Area, sq ft 0.71
    Exposed area above body, sq ft 0.37
    Aspect ratio 1.16
    Airfoil section . . . . NACA 0004-65
    Mean aerodynamic chord, $\bar{c}_t$, ft 1.05
    Length (moment center to 0.35 $\bar{c}_t$), ft 0.60
Body
    Length, ft 3.67
    Base area, sq ft 0.12
Moment center (on body center line)
    Horizontal location (aft of leading edge of M.A.C.) . . . . .   0.30$\bar{c}$
Ventral fin
    Area, sq ft 0.082

TABLE II.- ASSUMED MASS AND AERODYNAMIC PARAMETERS FOR

INERTIA COUPLING CALCULATIONS

Mass data
    Weight, lb   23,000
    I_Y, slug/ft^2   89,400
    I_Z, slug/ft^2   99,700
    $(I_X - I_Y)/I_Z$ 0.76
where I_X, I_Y, and I_Z are moments of inertia about the
    principal axes
Aerodynamic data, moment center at 0.28 $\bar{c}$
    C_{m_α}, per deg . . . .   -0.0041
    C_{n_β} . . . . (see fig. 13)
    C_{m_q} . . . .   -1.8
    C_{n_r} . . . .   -0.14
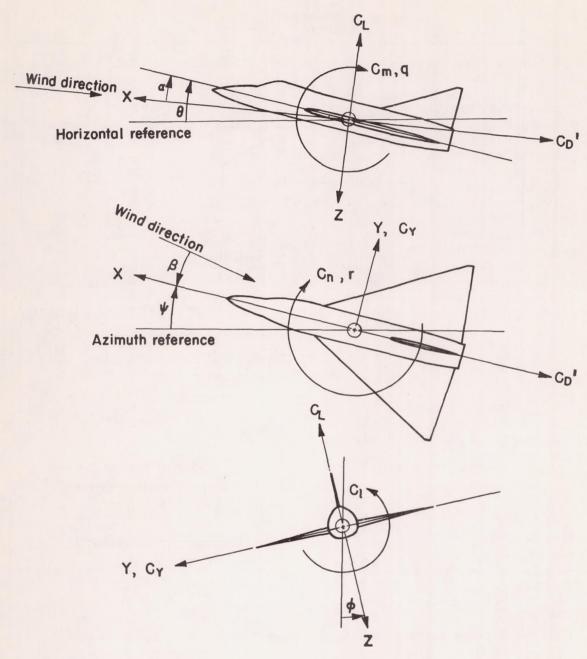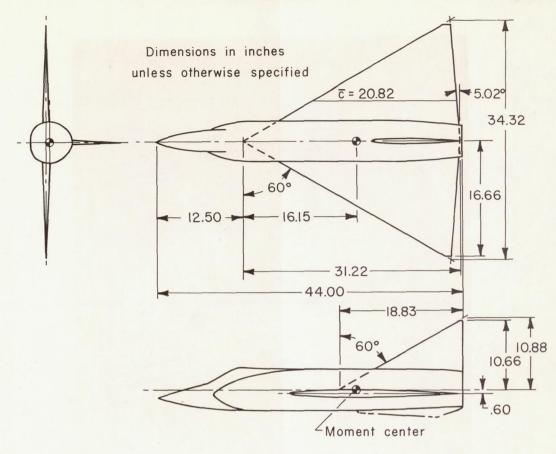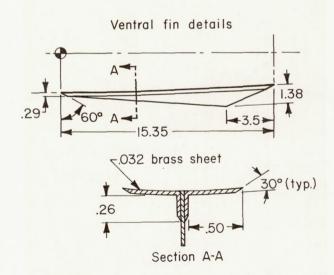
Figure 1.- The stability system of axes is an orthogonal system of axes having its origin at the center of gravity, the Z axis in the plane of symmetry and perpendicular to the relative wind, the X axis in the plane of symmetry and perpendicular to the Z axis, and the Y axis perpendicular to the plane of symmetry. Arrows indicate the positive directions of forces and moments.
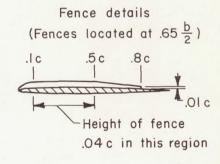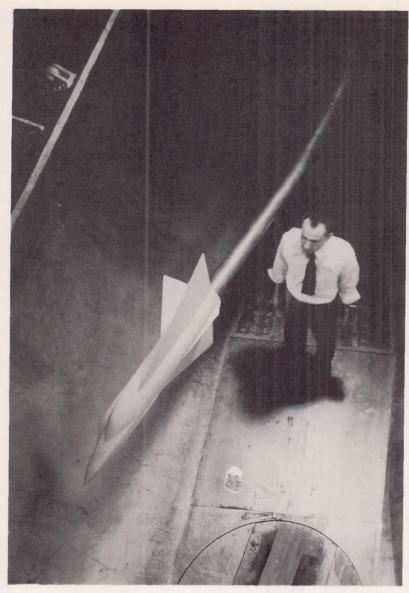
Dimensions in inches
unless otherwise specified

$\bar{c} = 20.82$

5.02°

34.32

60°

12.50   16.15

16.66

31.22

44.00

18.83

60°

10.88

10.66

.60

Moment center

Ventral fin details

.29

60°   A

A

1.38

3.5

15.35

.032 brass sheet

.26

30° (typ.)

.50

Section A-A

Fence details
(Fences located at $.65\frac{b}{2}$)

.1c   .5c   .8c

.01 c

Height of fence
.04 c in this region

Figure 2.- Geometry of the model.

CONFIDENTIAL

A-20880

Figure 3.- The model mounted in the wind tunnel.
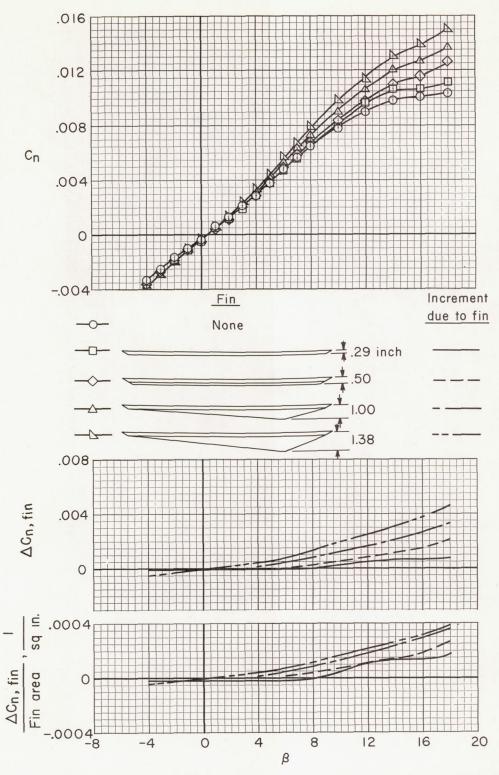
Figure 4.- The effects of several ventral fins on the yawing-moment coefficients of the model; M = 0.46, R = 4.9 million, α = 6°, wing on.

CONFIDENTIAL

(a) M = 0.25
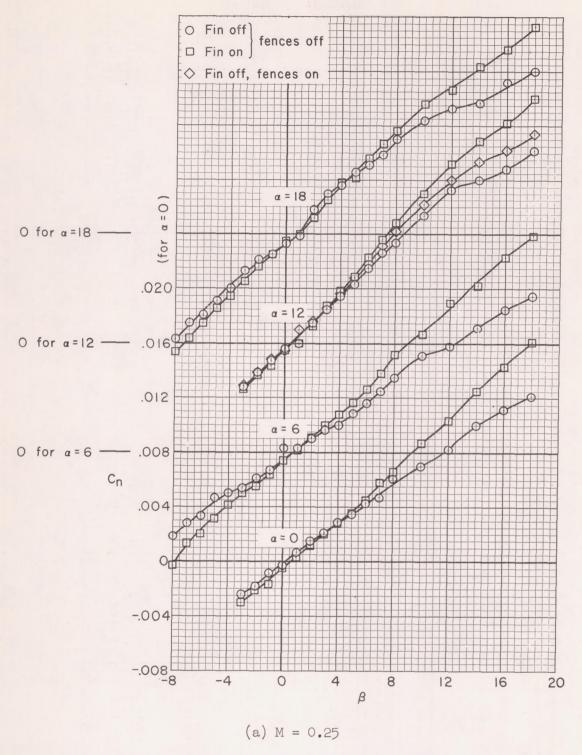
Figure 5.- The variation of yawing-moment coefficient with angle of side-slip; wing on.

(b) M = 0.80

Figure 5.- Continued.

(c) M = 0.90

Figure 5.- Continued.

(d) M = 0.94
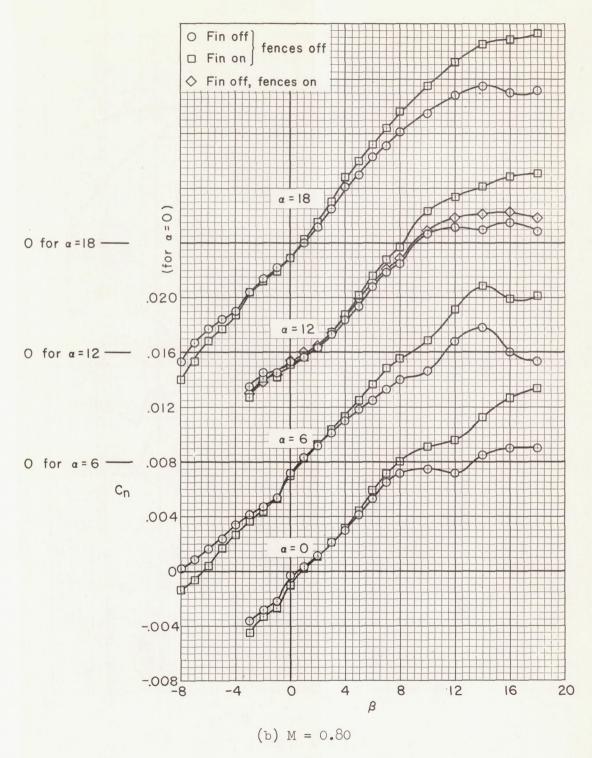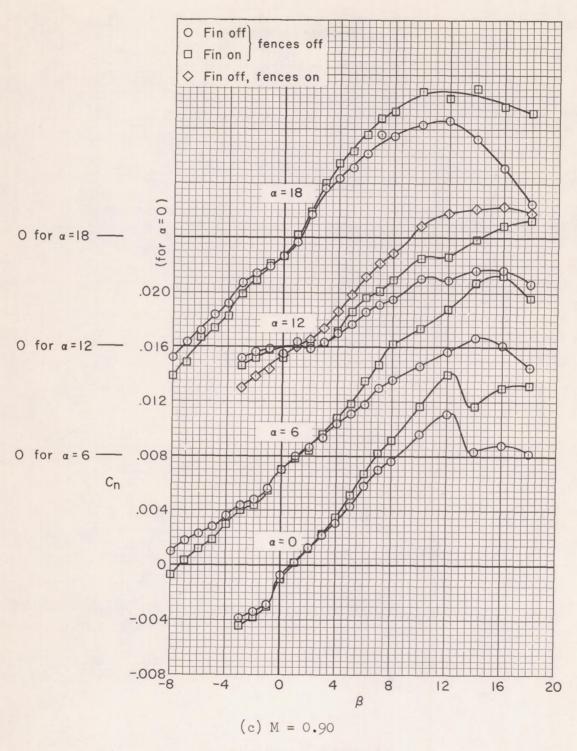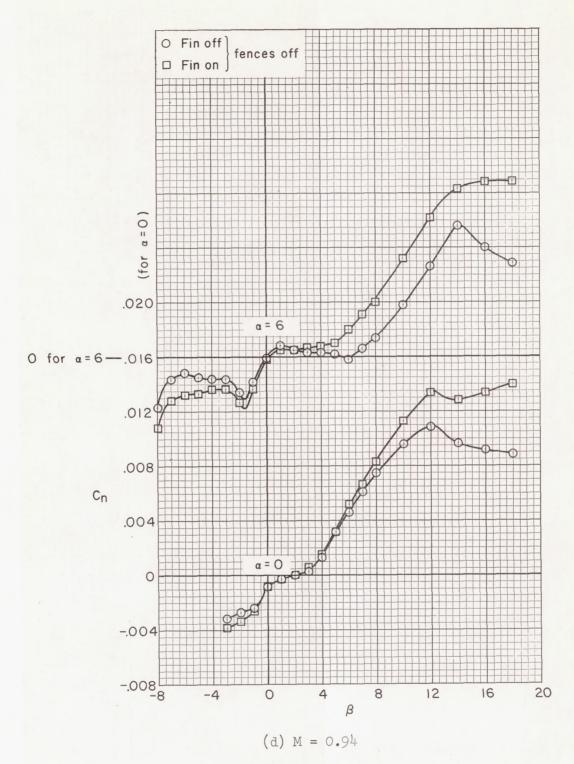
Figure 5.- Concluded.

(a) M = 0.25
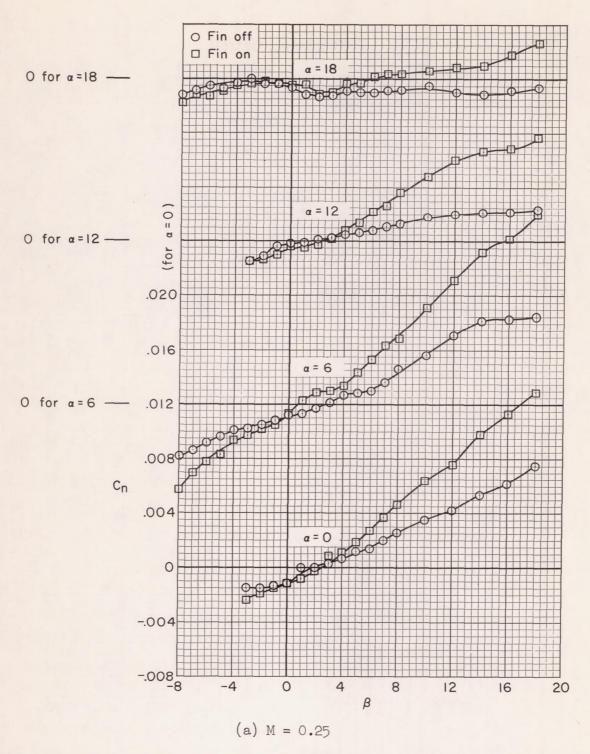
Figure 6.- The variation of yawing-moment coefficient with angle of side-slip; wing off.

(b) M = 0.80
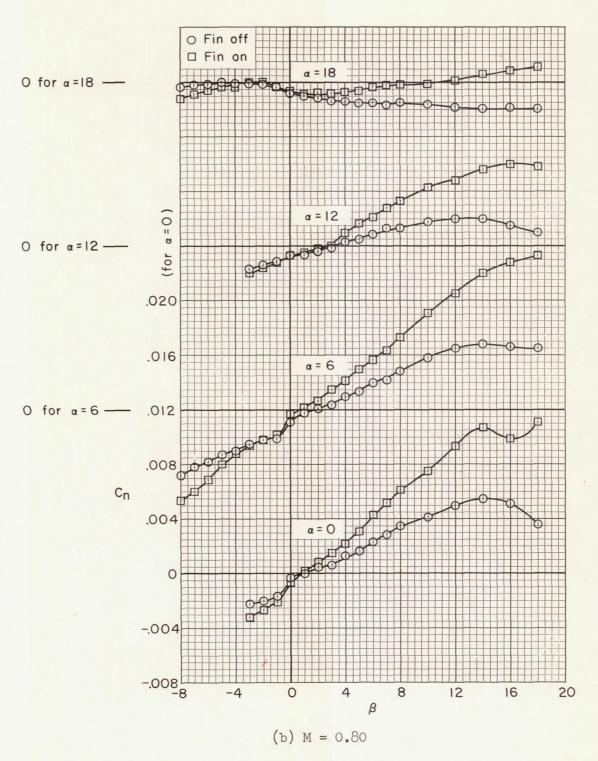
Figure 6.- Continued.

(c) M = 0.90
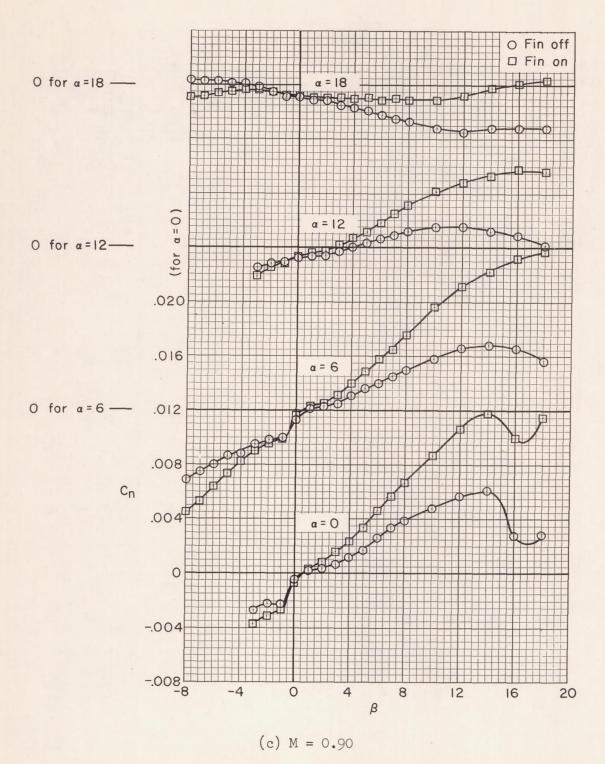
Figure 6.- Continued.

(d) M = 0.94
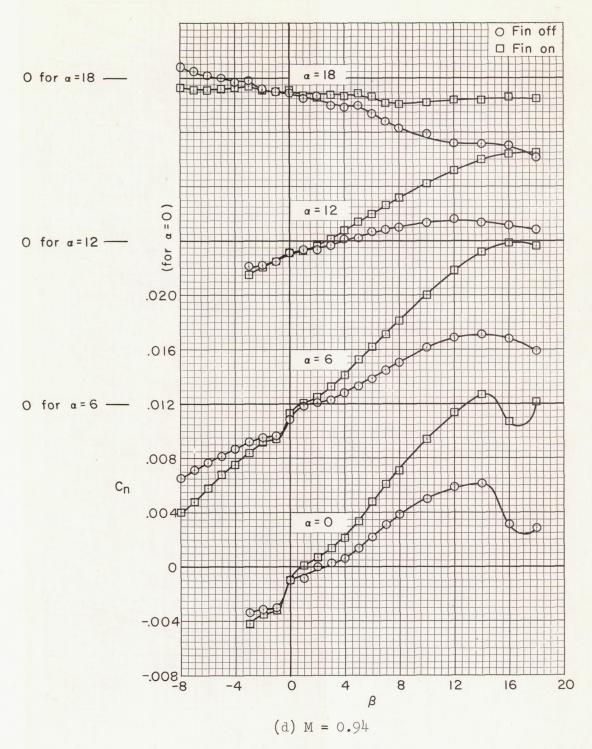
Figure 6.- Concluded.
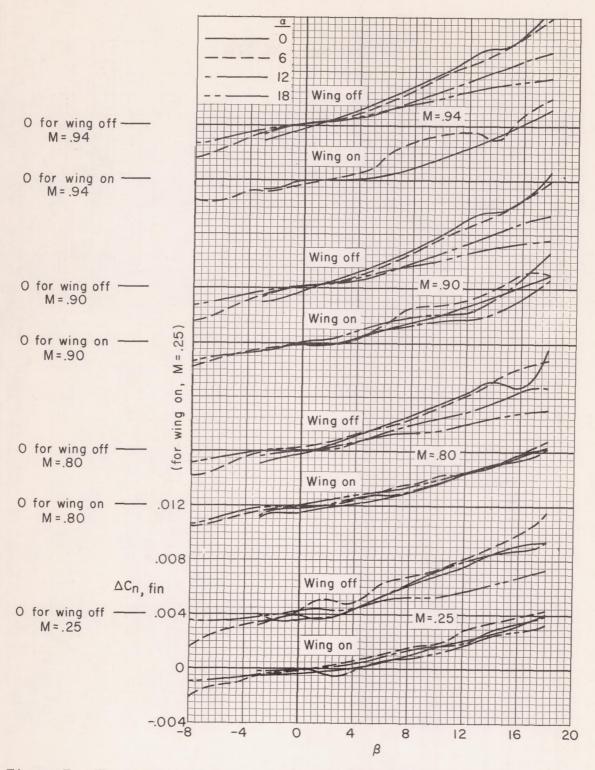
Figure 7.- The increment of yawing-moment coefficient due to the addition
of the ventral fin.
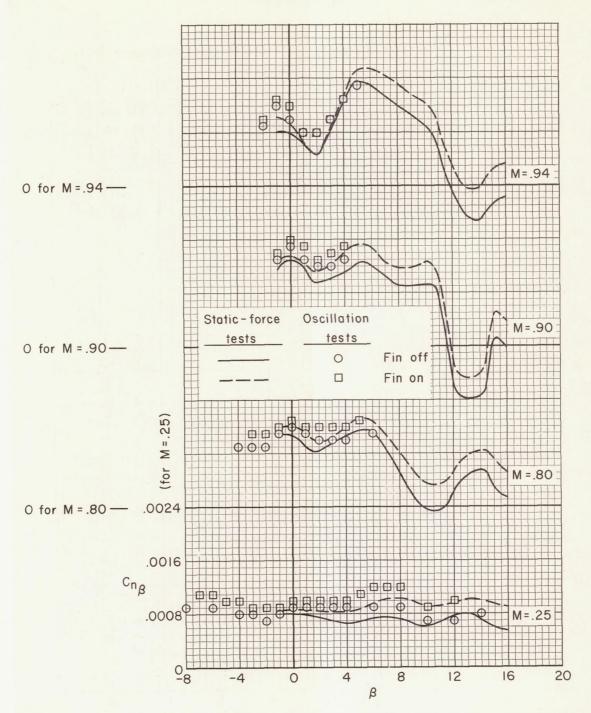
Figure 8.- The variation of directional stability with angle of sideslip;
$\alpha = 0$, wing on.
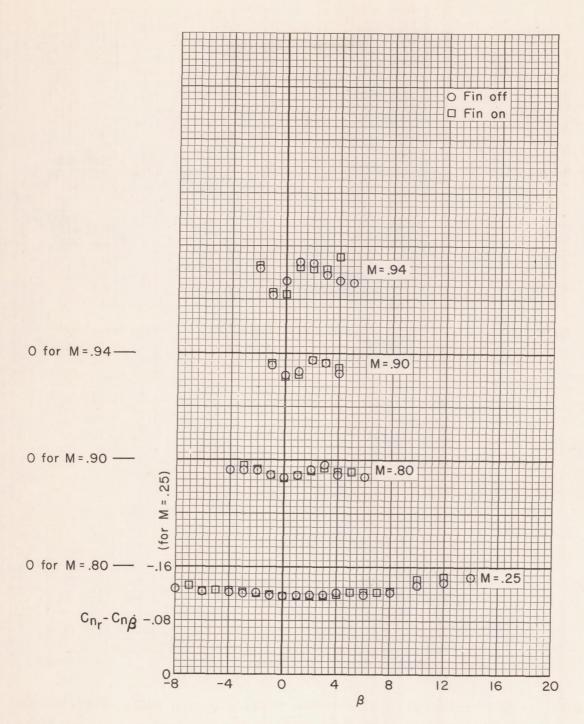
Figure 9.- The variation of damping in yaw with angle of sideslip; $\alpha = 0$, wing on.

(a) M = 0.25
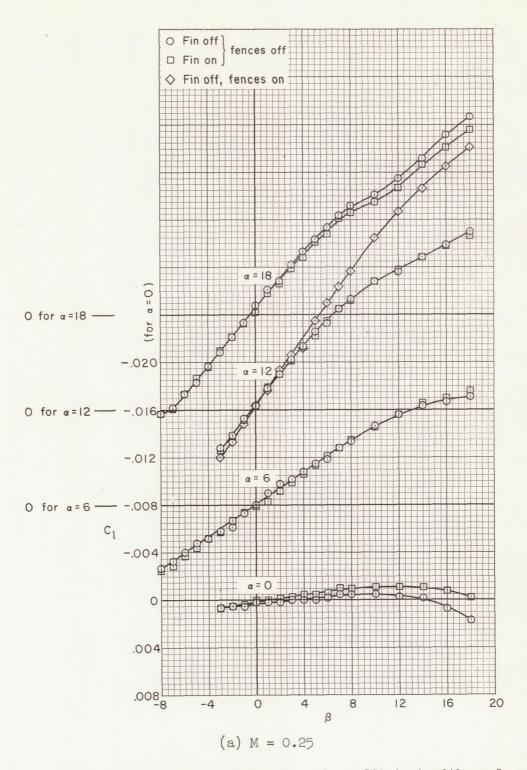
Figure 10.- The variation of rolling-moment coefficient with angle of
sideslip; wing on.

(b) M = 0.80

Figure 10.- Continued.

CONFIDENTIAL

(c) M = 0.90

Figure 10.- Continued.

CONFIDENTIAL

(d) M = 0.94
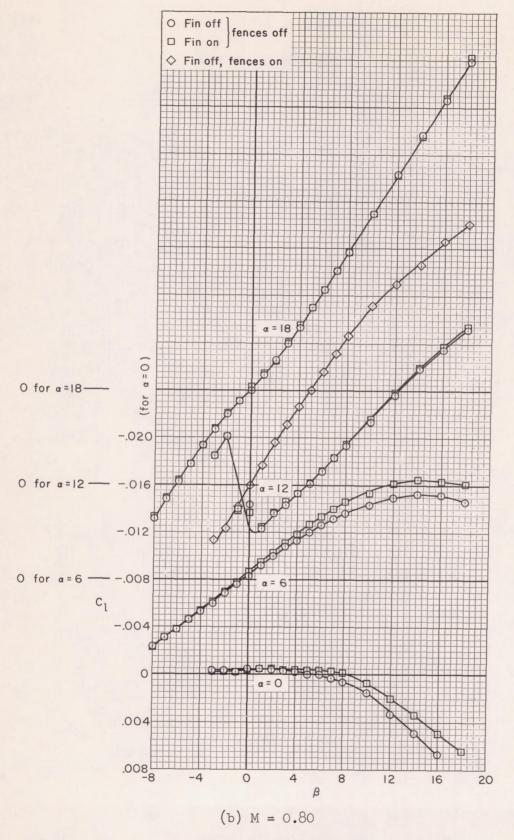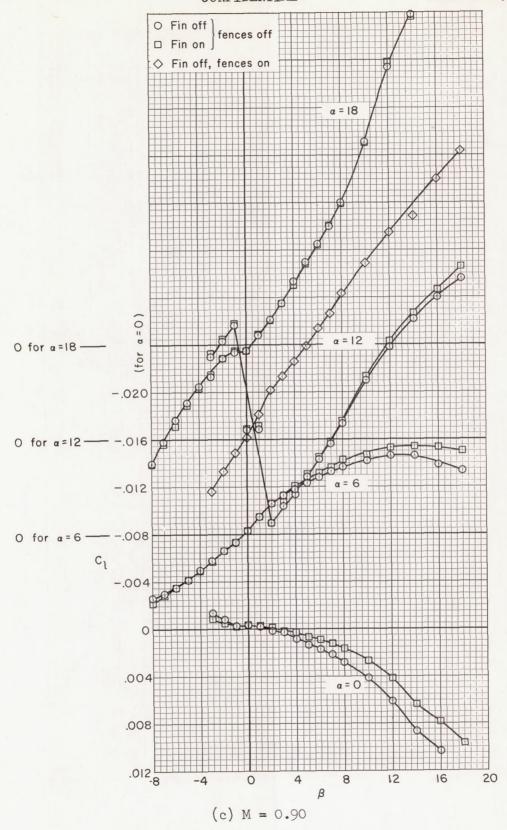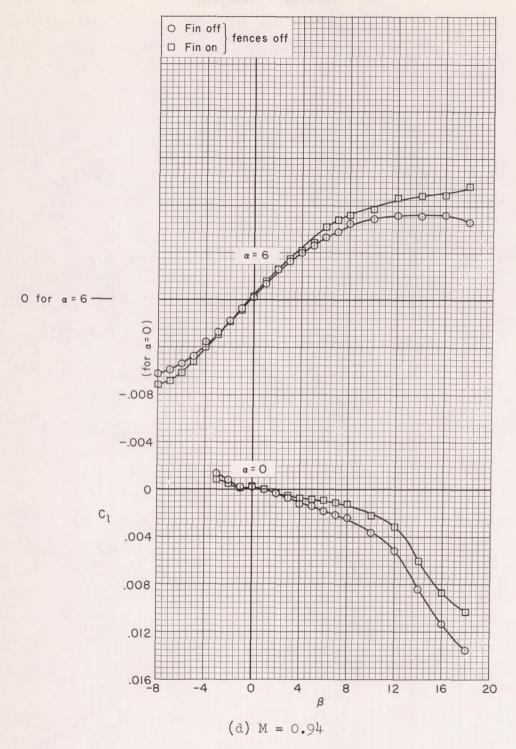
Figure 10.- Concluded.

(a) M = 0.25
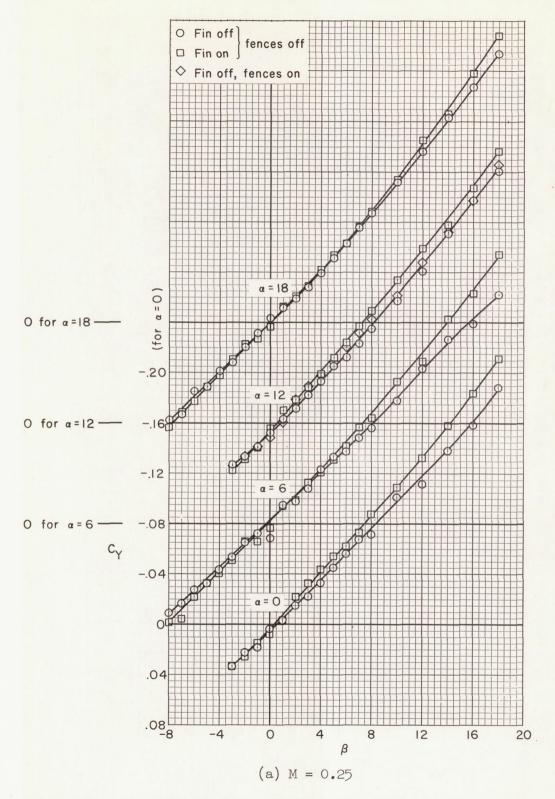
Figure 11.- The variation of side-force coefficient with angle of side-slip; wing on.

(b) M = 0.80

Figure 11.- Continued.

(c) M = 0.90

Figure 11.- Continued.
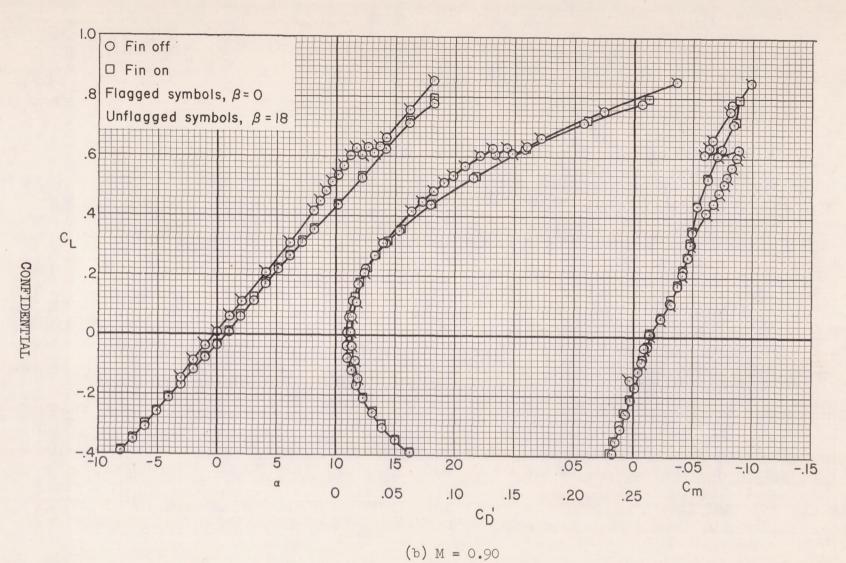
(d) M = 0.94
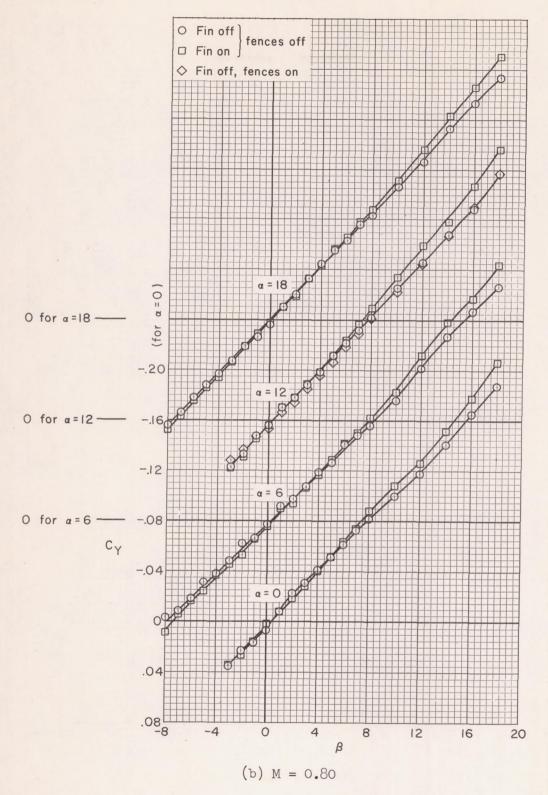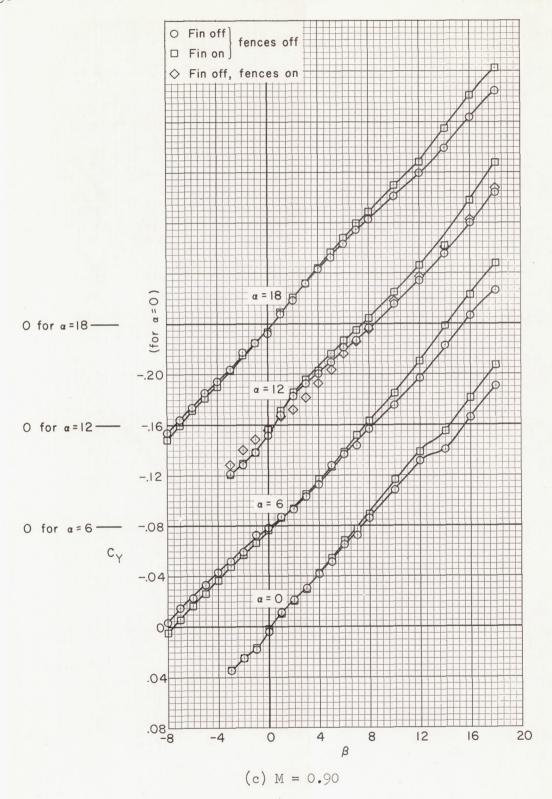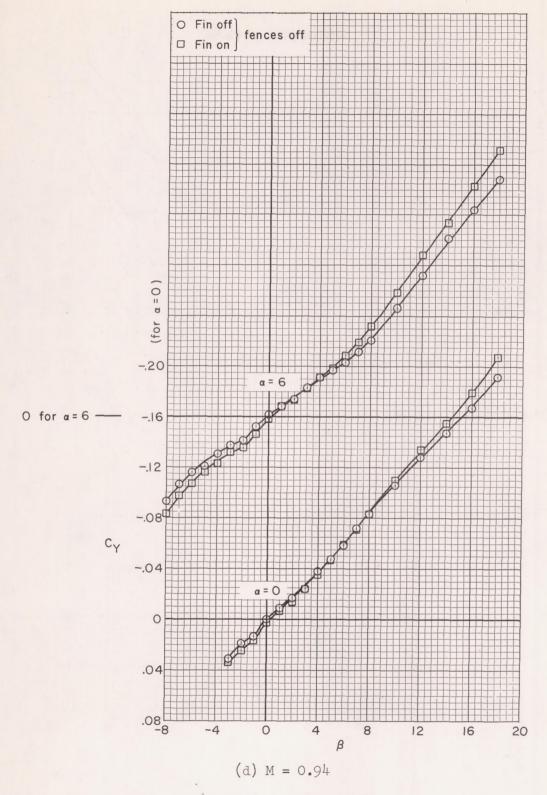
Figure 11.- Concluded

(a) M = 0.25
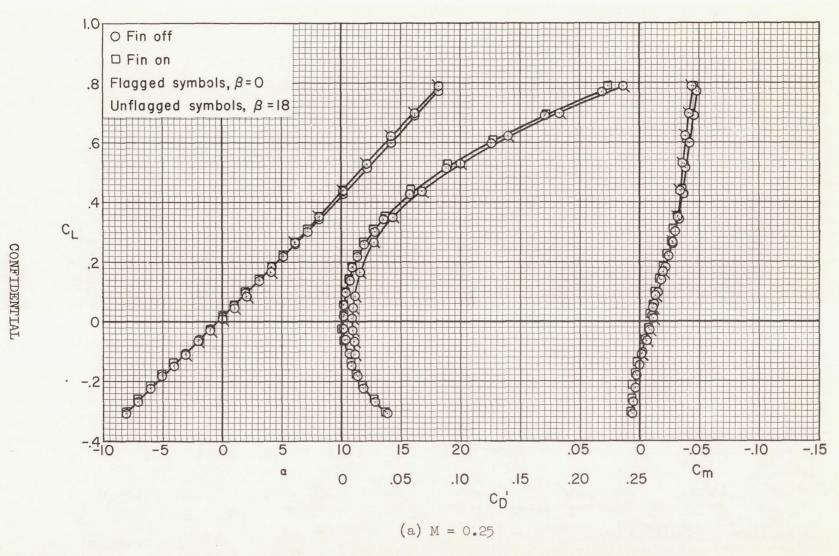
Figure 12.- The longitudinal characteristics of the model; wing on.
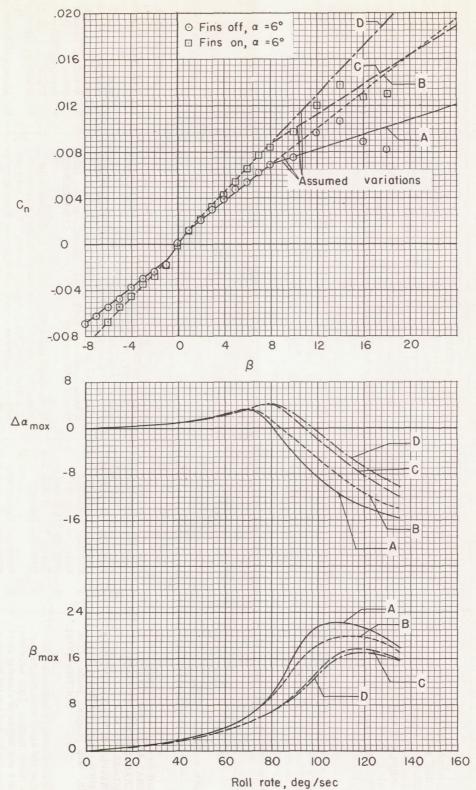
(b) M = 0.90

Figure 12.- Concluded.

Figure 13.- Several assumed variations of yawing-moment coefficient with sideslip and the corresponding calculated response to steady rolling of an airplane free to pitch and to yaw; M = 0.80, altitude = 40,000 ft.

CONFIDENTIAL